Adapting Mechanical Characterization of a Biodegradable Polymer to Physiological Approach of Anterior Cruciate Ligament Functions

A. Rangel, L. Colaço, N.T. Nguyen, J.-F. Grosset, C. Egles, V. Migonney

Adapting mechanical characterization of a biodegradable polymer to physiological approach of Anterior Cruciate Ligament functions

André Rangel[a*], Laila Colaço[b], Ngoc Tuan Nguyen[a], Jean-François Grosset[b], Christophe Egles[b], Véronique Migonney[a]

[a] Laboratoire de Biomatériaux pour la Santé (LBPS), Laboratoire de Chimie, Structures, Proprietés de Biomatériaux et d'Agents Thérapeutiques (CSPBAT), UMR CNRS 7244, Université Sorbonne Paris Nord, France

[b] Alliance Sorbonne université, Université de technologie de Compiègne, CNRS, UMR 7338 BioMécanique et BioIngénierie (BMBI), Centre de recherche Royallieu, CS 60 319, 60 203 Compiègne cedex, France

*Corresponding author: Laboratoire de Biomatériaux pour la Santé (LBPS), 99, avenue Jean Bapiste Clement, Villetaneuse, Université Sorbonne Paris Nord, France. Email : andre.luizreisrangel@univ-paris13.fr

Abstract

Background and objective

Over the past decades, anterior cruciate ligament injuries have become a considerable public health issue. Due to specific physiological conditions such injuries often demand replacement surgery and can take up to two years to a complete recovery. Using biomaterials able to accelerate the healing process could represent a remarkable progress in the field. The main goal of this article is, therein, to evaluate the mechanical properties of poly(ε-caprolactone) (PCL) fibers with biological properties enhanced by poly(sodium styrene sulfonate) (PNaSS) grafting when subjected to mechanical stress in different conditions.

Materials and methods

PCL fibers were thermal grafted with PNaSS. The grafting density was estimated by the toluidine blue colorimetric assay (TB). The influence of the grafting on in vitro primary ACL fibroblast behavior was evaluated by cell proliferation and fluorescence microscope images. The mechanical behavior was evaluated by tensile experiments in air and water, fatigue experiments and simulated walk efforts.

Results

The results show that poly(ε-caprolactone) bundles have their mechanical behavior changed by the different surface treatments and nature of mechanical stress. Although, compared with the values of the natural ligament, the poly(ε-caprolactone) has shown superior mechanical properties (Young's Modulus, elastic deformation and ultimate tensile stress) in all studied scenarios. In addition, the pNaSS-grafted surfaces presented a positive influence in the cell proliferation and morphology.

Conclusion

The pNaSS-grafted PCL has responded mechanical and biological requests for suitable ligament prosthesis material and could be considered as a promising alternative for ACL reconstruction.

Key-words: Anterior Cruciate Ligament, biodegradable polymer, surface functionalization, mechanical characterization, walking simulation.

1. Introduction

Anterior cruciate ligament (ACL) partial or total ruptures have become more frequent in recent years with the popularization of intense sports activities. In the USA, over 100,000 ACL medical procedures are performed each year, an incident rate of 1/3000 [1]. Unfortunately, in the case of a complete rupture, the spontaneous healing process is almost impossible [2]. Given this problem, different techniques and biomaterials have been used to replace the functions of the ACL [2 - 4]. However, the poor choices of materials for the first generation of prosthesis, especially carbon and PTFE based [5], led to problems related to both mechanical behavior and biocompatibility such as ligament rupture and fixation issues, debris amassing, bone tunnel enlargement and inflammation [4, 6, 7] . In response to this failure, synthetic prostheses were developed using polymers, mainly poly(ethylene terephthalate) (PET) [8]. However, PET ligaments still have limitations in biointegration and mechanical properties [9], and most importantly, face a strong resistance from healthcare professionals.

At this point, finding a slowly degradable biomaterial that combines good biocompatibility and mechanical properties similar to the natural ligament has become the key point of several studies [10 - 14]. In this context, the tissue engineering field started working towards developing an innovative type of prosthesis serving as a

support for a new ligament growth [15, 16]. The objective is to use biodegradable material to guide the generation of a new tissue that gradually replaces it [17]. Therefore, to reduce the problems of tissue regeneration due to the constraints realized over the prosthesis, it is necessary that the synthetic ligament gradually loses its rigidity and while the newly formed ligament gains it [8]. Only few materials are able to fulfill all these stipulations and a fortuitous example is the Poly(caprolactone). This semi-crystalline and biodegradable polymer presents total degradation time as high as four years depending on the starting molecular weight [18 - 20] and is a promising candidate for long-term implantable applications, due to its compatible mechanical properties such as Young's Modulus, elastic deformation and rupture strength and well-known biocompatibility [21].

Nevertheless, besides the relevance of these bulk properties, the success of a prosthesis implantation in the biological environment is closely linked to surface characteristics and different surface treatments were proposed to increase polymeric prosthesis efficiency, such as glow discharge treatments, plasma assisted modifications or grafting with bioactive molecules, which allows positive interaction with the body [22].

Poly(sodium styrene sulfonate) (PNaSS) grafting of implants surfaces has demonstrated a positive influence on the cell response, over several surfaces for both in vitro and in vivo assays [23 - 26]. Significant results were obtained for PET ligaments in terms of cell spreading and cell adhesion strength [27, 28] and the same tendency has been verified for poly(ε-caprolactone) PNaSS grafted samples [29].

Concerning the mechanical properties of PNaSS grafted poly(ε-caprolactone), a previous study has shown that poly(ε-caprolactone) fibers present suitable behavior with superiors Young modulus, elastic deformation and ultimate tensile stress (UTS) when

compared to native ACL values [29]. However, the mechanical tests carried out during this study didn't consider the nature of the efforts that ACL is subject to daily, making additional tests necessary to complement the characterization.

Simulating real situations of the ligament in the knee joint is a way to come closer to physiological conditions and a strongly relevant option to mechanical characterization of artificial ligaments. The present study aims to go deeper into the mechanical characterization of the artificial ligaments material, before and after surface functionalization, by performing tests in different environments and mechanical solicitations modes. Poly(ε-caprolactone) fibers were then subjected to tensile tests in an aqueous environment, fatigue tests and a new protocol was established: the walk cycle experiment.

2. Material and methods

2.1 Samples Preparations

The poly(ε-caprolactone) bundles were assembled from 20 poly(ε-caprolactone) fibers (MDB Texinov, France). The fibers were 100 µm diameter and the bundles were delimited by handmade ties. To eliminate the spin finish components the bundles were submitted to ethyl ether Soxhlet extraction (6 h at 30 °C). Spin components free poly(ε-caprolactone) bundles were then PNaSS grafted. This operation was carried out in two steps: surface activation in by ozonation (BMT 802 N ACW, oxygen flow rate of 0.6 L/min) at 30°C in distilled water for 10 min; and radical polymerization of NaSS from the surface (0.7M H_2O) at 45 °C for 1 h.

All samples were washed in distilled water for 48 hours and dried under vacuum before assays.

2.2 Materials characterization

2.2.1 Toluidine Blue colorimetric assay

The PNaSS grafting density was assessed using the toluidine blue O colorimetric assay. The method was previously described before by Helary et al. [30]. Briefly, samples were soaked in 5 mL of toluidine blue O (TB) 50mM aqueous solution (Roth Sochiel, Germany) and kept at 30°C for complexation reaction. After 6 hours the samples were washed three times in 1mM NaOH aqueous solution for 5 min. Finally, each sample was transferred to a vial containing 2mL of aqueous acetic acid solution (50%, v/v) and kept at room temperature for 24 hours of decomplexation. The absorbance (abs) of the resulting solution was measured by UV/visible spectroscopy (Perkin Elmer Lambda 25 spectrometer, Waltham, USA) at 633 nm and compared to a standard curve of known TB concentration. The grafting density (GD) in mol/g was calculated following Equation 1:

$$GD = \frac{abs\ V}{\varepsilon\ l\ S}$$

The aqueous acetic acid volume is called V (L), ε is the angular coefficient of toluidine blue standard curve solution (L/(mol cm)), l is the length of the spectrophotometer path length (cm), and S is the surface area of the samples (cm^2).

2.2.2 Differential Scanning Calorimetry

For the thermal characterization, 2 mg of fibers were positioned in an aluminum crucible and placed into a DSC 8000 calorimeter (Perkin Elmer, USA) under nitrogen atmosphere. All scans were performed from -75 to 100 °C, at 10 °C/min. The crystallinity degree was estimated as a ratio of melting enthalpy of the samples (ΔH_m)

and melting enthalpy of 100% crystalline poly(ε-caprolactone) (ΔH_{m0}) [31] as showed in the equation 2.

$$Xc = \left(\frac{\Delta Hm}{\Delta Hm0}\right)100$$

2.2.3 Atomic Force Microscopy

The topography of the polycaprolactone fiber surface was observed by AFM MultiMode 8 (Bruker, Billerica, USA) and analyzed by NanoScope Analysis 1.8 (Bruker) using the method ScanAsist in the air (f= 0.5 kHz, 0.5 μm x0.5 μm and 5 μm x5 μm scans). A single tip was used (k = 0.4 N/m, tip radius < 10 nm) for the measurements. Peakforce QNM was used to map the adhesion (room conditions) and absolute calibration was used. Gaussian fix was used for calculate the adhesion force.

2.3 Cell culture

Before cell culture the samples were widely washed in salt solution (NaCl 1.5M, NaCl 0.15M and PBS), rinsed in ethanol 70% v/v solution for 20 minutes and irradiated with UV under a flow hood for 15 minutes each side. The samples were then conditioned in DMEM for 8 hours and stored in complemented DMEM (10% Bovine fetal serum, 1% streptomycin-penicillin, 1% L-glutamine) overnight at 37 °C. Anterior cruciate ligaments cells (sACL) were isolated from a Merino sheep (2-year old female) in accordance with the German legislation on protection of animals and the NIH Guidelines for the Care and Use of Laboratory Animals (NIH Publication 85-23, Rev. 1985). The sampling was, as well, approved by the local governmental animal care committee. For isolate the cells, the tissue were cut into of 1 mm² pieces, washed in PBS three times, and incubated for 6 h in 0.1% w/v collagenase solution at 37°C under 5% CO_2. The suspension was centrifuged 3 min at 1,500 rpm, the supernatant was

disposed, the cells suspended in complete DMEM and cultured in T-75 flasks until confluence. All experiments were performed with cells under passage 5.

2.3.1 Cell proliferation

Grafted and non-grafted samples were placed in a 24 wells plate and seemed with 1ml of cell suspension (50,000 cells/ml). The plates were incubated at 37°C under 5% CO_2 and cultured for 1, 3 and 7 days, changing the culture media every 48 hours. After each point was reached the samples were rinsed twice in PBS, transferred to a new well. The cells were detached by trypsination and counted using a Scepter Cells Counter (Merck, USA).

2.3.2 Cell morphology

The cell morphology over grafted and non-grafted samples was evaluated by fluorescence microscopy after 24 hours of culture. The samples were rinsed in PBS and fixed in 4% formaldehyde solution for 10 minutes at room temperature. The samples were then rinsed in PBS three times and stained with 4′,6-diamidino-2-phenylindole (DAPI, 1/500 dilution) and fluorescein isothiocyanate (FTIC, 0.13 mg/ml) for 5 minutes at room temperature. The samples were once again rinsed in PBS three times, allowed to dry and the images were acquired using a LSM 710 confocal laser scanning microscopy (Zeiss, Germany).

2.4 Mechanical characterization

2.4.1 Tensile experiments

Tensile experiments were realized using a Bose Electroforce 3230 test instrument (Bose, USA) with a 450 N force sensor. Poly(ε-caprolactone) bundles submitted to classic traction assays were assembled from 20 fibers (100 µm diameter).

The cross section was calculated by multiplying the cross-section of a single fiber by twenty. The samples were positioned between the grips (effective length = 10mm) and charged until total rupture. The loading speed was set in 0.06 mm/s. Stress-strain curves are recorded and the following parameters were calculated: Young Modulus, Yield stress, elastic deformation, ultimate tensile stress (UTS) and ultimate strain.

2.4.2 Aqueous environment assays

For this series of experiments a sealing recipient (5L capacity) was positioned around the grips of the Bose Electroforce 3230 test instrument. The samples were placed and the recipient filled with water at 4 different temperatures (25, 33, 37 and 40 ° C). All tested temperatures are above the PCL glass transition temperature (-60° C) [32]. From this point, traction tests were performed following the same protocol used for traction experiments described above.

2.4.3 Fatigue experiments

The samples were subjected to 1,000,000 sinusoid cycles of charge using the Bose Electroforce 3230 test instrument. The cycles were performed at 3 and 5 Hz with displacement controlled for 10 and 15% of the samples length. The deformation values were stablished based in the ACL elongations during 90° bending movements (as in the sit motion) and overflexion (120 °) previously reported [33]. The stress/number of cycles curve (S-N curve) was normalized by the initial stress and the rate of resistance loss was evaluated.

2.4.4 Walk Cycle experiments

The Bose Electroforce 3230 test instrument was programed to perform the following protocol, aiming to emulate the movements of ligament elongation and relaxation during the walk phases by considering an average pace of 1.528 m/s or 5.5

km/h [33]. The march was divided in two main phases: the support or stance phase (60% of the time or 0.312 seconds) and the oscillating or swing phase (40% of the cycle or 0.208 seconds). The support phase was divided into 3 stages: during the double reception support phase (0.052 seconds) the samples were stretched by 1.7%, then for the single-limb support phase the the samples were relaxed by 1.7% (0.0624 seconds) to remain unsolicited for 0.1456 seconds and then stretched by 4.3% during the double propulsion phase (0.052 seconds). The oscillating phase was divided into two stages (0.104 seconds each): in the first, the samples were stretched by 5.84% and then relaxed by 10.46% for the second one.

Fig 1 shows the phases of the walk with their duration and the elongation of the ACL according to the degree of flexion of the knee [33]. After simulating this cycle for 30 min, the poly(caprolactone) samples were subjected to a tensile test loading at 0.06 mm/s until total rupture.

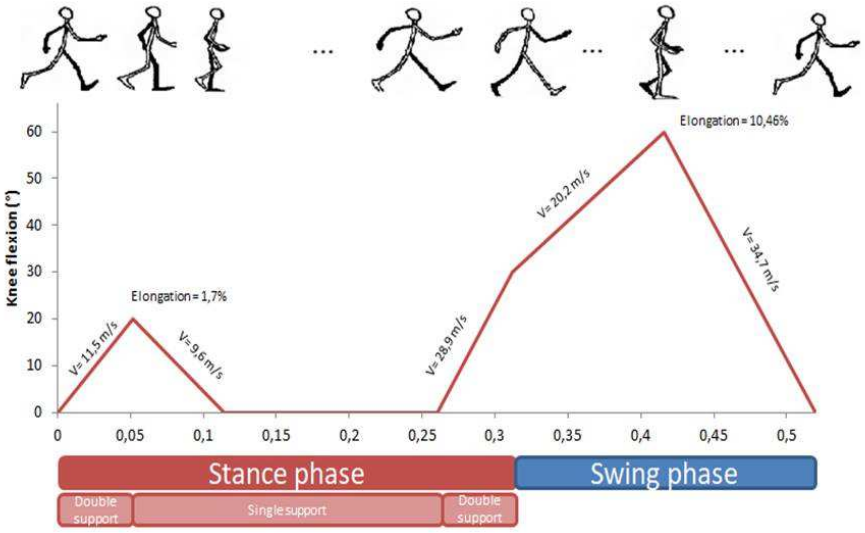

Fig 1. Schematic representation of ACL's elongation during the phases of gait. Inspired by Mark Dutton [35].

2.4.5 Statistical analysis

All physical-chemical and biological characterization assays were performed in triplicate (n=3), mechanical characterization assays were performed at least 5 samples for each studied group. All presented statistical differences between mean values were calculated with One-Way ANOVA test using excel software ($\alpha < 0.05$).

3. Results and discussion

3.1 Materials Characterization

The TB assay confirmed the PNaSS grafting of poly(ε-caprolactone) fibers, as well as the negligible value of non-specific stain absorption for non-grafted samples. The values of 142.9 ±0.8 nmol/cm^2 for grafted fibers against 10.1 ±0.1 nmol/cm^2 for control reaffirm the effectiveness of the surface treatment.

The DSC thermograms revealed no remarkable changes in the thermal properties of the fibers over the treatment. As can be seen in Fig 2 a small increase of crystallinity and fusion temperature (Tf) can be verified in fibers after spin finish removal, however it was not statistically relevant since the variation approximates the values to the same. In addition, the crystallinity increases after thermal grafting treatment.

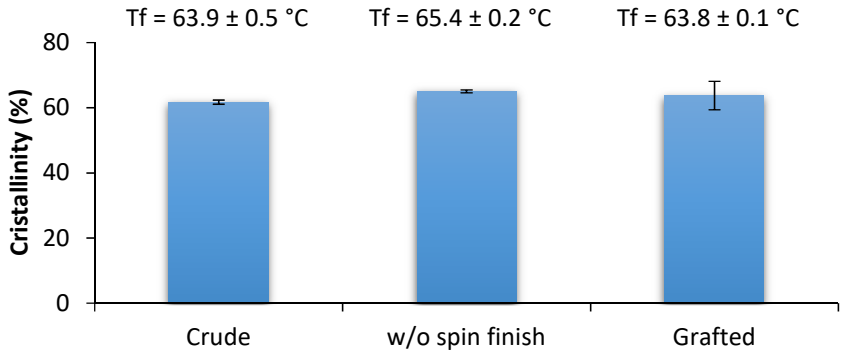

Fig 2. Crystallinity and fusion temperature of as received, after spin finish removal and grafted poly(ε-caprolactone) samples (n=3, $\alpha < 0.05$).

The surfaces of fibers were scanned at 5 µm x 5 µm (25ºC, f = 0.5Hz, in the air). Fig 3a shows a layer of industrial spinning lubricant over crude samples. This layer has from 120 to 180 nm thickness. After spin finish removal and thermal grafting no oil was

found over the surfaces and a fibril structure can be noted (Fig. 3b and 3c zoom). No statically difference was observed in the roughness of the studied groups.

The Fig. 3d, 3e and 3f show the adhesion map between the tip and the fibers. A reduction of the adhesion force was verified after each step of the treatment: 24% average reduction after SFR (from 8.12 to 6.14 nN) and 49% after thermal grafting (from 8.12 to 4.11 nN). The residual stress on polymeric surfaces has been reported to increase the contact force between tip and material [36]. In the case of the PCL fibers the residual stress can be alleviated by the temperature of the spin-finish removal and grafting, decreasing therefore the adhesion force.

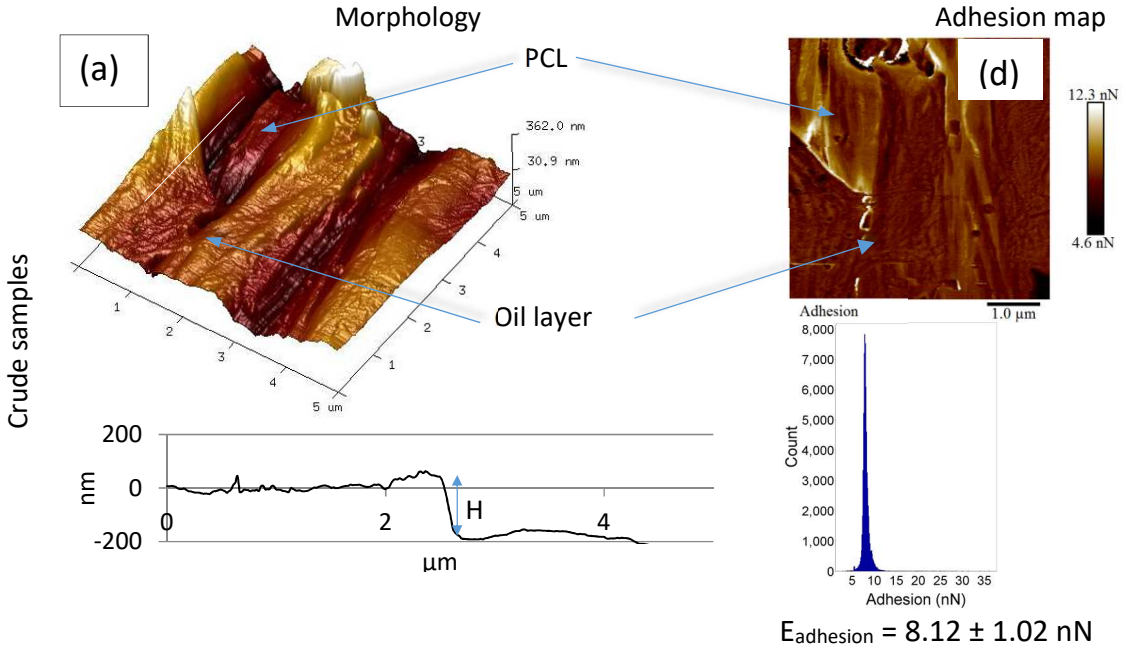

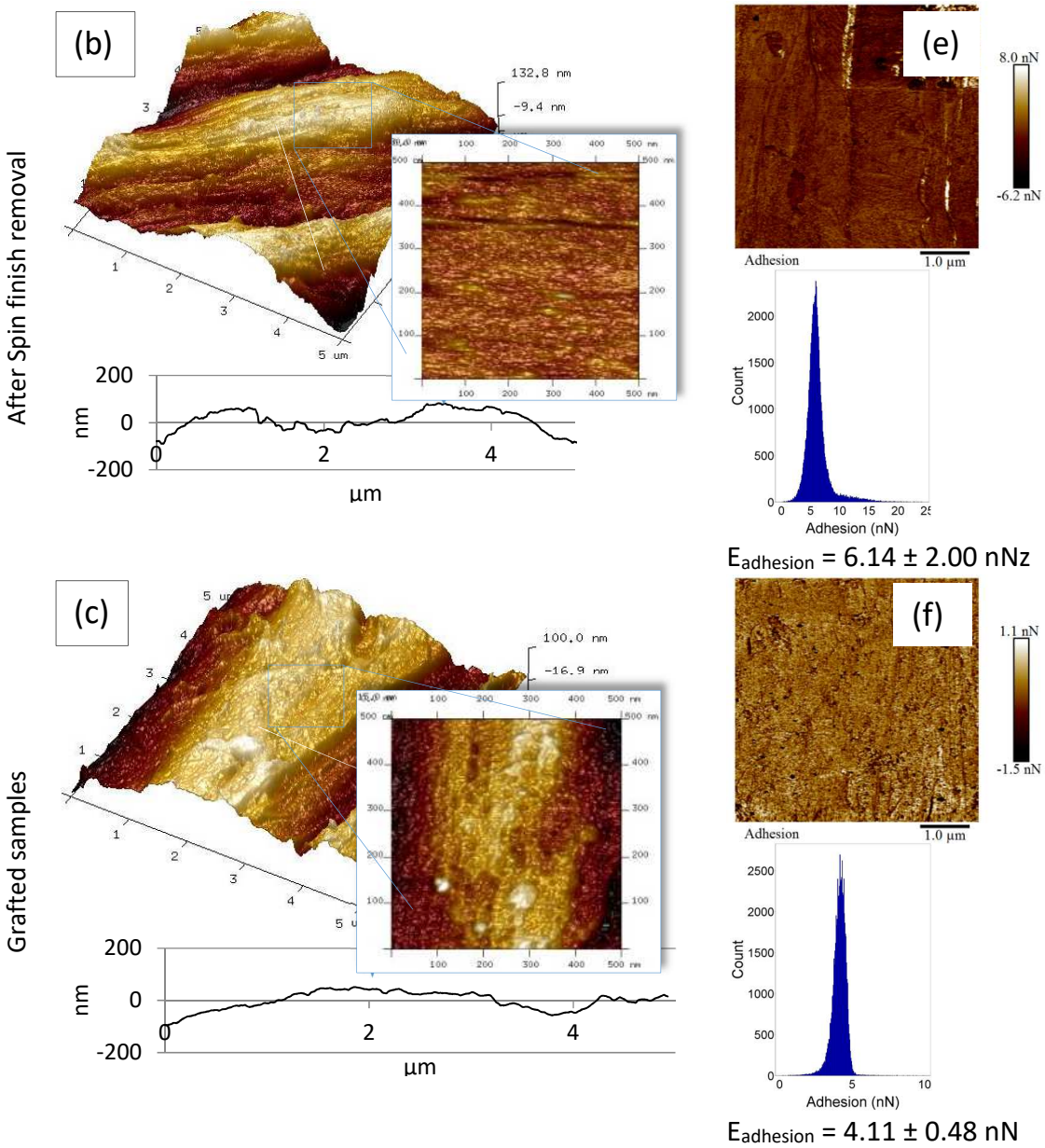

Fig 3. Topography of polycaprolactone fiber at 5x5 µm scanning area. (a) crude poly(ε-caprolactone) fiber; (b) poly(ε-caprolactone) after spin finish removal; (c) PNaSS grafted poly(ε-caprolactone) fiber. The "zoom in" of the images b and c cover 500x500 nm area. The Adhesion map, adhesion force distribution and values (3 different over 3 samples per group) for crude samples, after spin finish removal and PNaSS grafted are showed in figure 3d, 3e and 3f respectively .

3.2 Cell culture

The cells counting showed the influence of the PNaSS presence on cell proliferation over the poly(ε-caprolactone) fibers. As seen in the Fig. 4, after 24 hours of cell culture a significant superiority on the cell number was verified for grafted

samples against non-grafted surfaces. This trend was confirmed for days 3 and 7 with; at least, three times more cells for the grafted group when compared to the non-grafted.

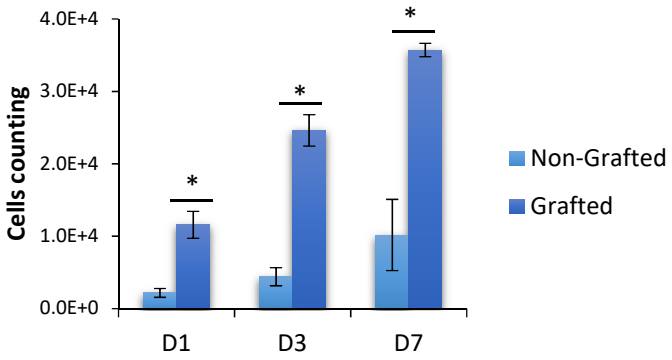

Fig 4. s(ACL) proliferation over grafted and non-grafted samples after 1, 3 and 7 days of culture (n=3, $\alpha < 0.05$).

The fluorescence images (Fig 5) confirm the positive influence of the PNaSS on cell behavior after 24 hours of cell culture. Besides the superior number, a higher cell spreading was also verified on grafted sample (Fig 5A).

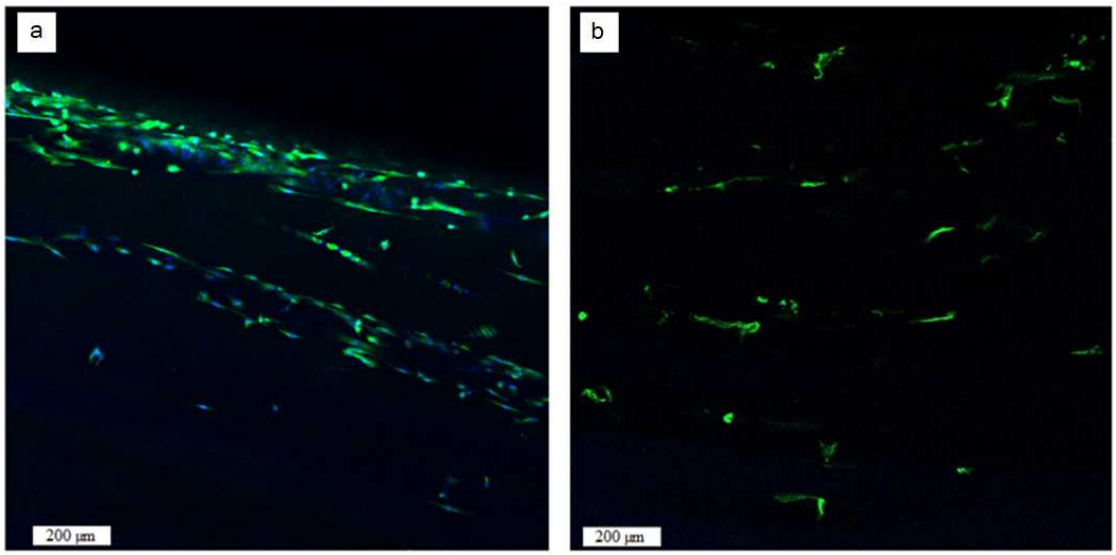

Fig 5. Fluorescence microscope images of s(ACL) primaries cells on a) grafted and b) non-grafted poly(ε-caprolactone) samples.

As matter of fact, the PNaSS has been linked to early signaling of important adhesion and spreading pathways (FAK phosphorylation and MAPK cascade) [24] creating a favorable environment to cells development. These preliminary results of cell

culture support this statement and ratify the previously verified distinguished cell attachment on grafted poly(ε-caprolactone) [25, 26, 29, 37].

3.3 Mechanical Properties

3.3.1 Influence of the grafting process on the mechanical characteristics of poly(ε-caprolactone) bundles

Young modulus (E), elastic strain (ε), Yield Stress, ultimate tensile stress (UTS) and ultimate strain were determined for poly(ε-caprolactone) crude bundles and after spin finish removal and pNaSS thermal grafting. Table 1 summarizes the results of the fibers for different conditions.

Table 1. Mechanical data obtained from traction experiments (n = 5) and reference native ACL values [5].

	Young's Modulus (MPa)	Yield Stress (MPa)	Elastic Strain (%)	Ultimate Tensile Stress (MPa)	Ultimate Strain (%)
Crude bundles	961 ± 49	312 ± 11	21 ± 2	354 ± 29	80 ± 12
Bundles without spin finish	789 ± 60	265± 21	28 ± 1	297 ± 32	96 ± 12
Bundles after thermal grafting	717 ± 64	254 ± 22	31 ± 1	280 ± 17	76 ± 14
Native ACL (male/female)	163/149	-	10–15/10-15	36.4/31.5	36 /35

Crude poly(ε-caprolactone) bundles showed the highest value for Young modulus (961 ± 49 MPa) with an elasticity of 21 ± 2% and a UTS of 354 ± 29 MPa.

After spin finish removal both Young modulus and the UTS decreased, 18% (789 ± 60 MPa) and 16% (297 ± 32 MPa) respectively, while the elastic deformation was 33% higher (28± 1%).

The same tendency was verified and amplified after the PNaSS grafting process. The Young Modulus was 25% smaller than the original value (717 ± 64) and a decrease of 21% for UTS (280 ± 17) was verified. As expected, the elastic strain was higher (31

± 1%) than for crude PCL. The reduction of the Young modulus can be explained by the heating performed in both removal of spin finish components and thermal grafting. The wires fabrication process include sudden temperature variation, which was reported as responsible for create residual tension on polymers [38, 39] and increasing the Young's modulus. Although no significant changes were verified in the crystallinity after spin finish removal and grafting (Fig. 2), as seen in the adhesion energy decrease verified by AFM analysis (see Fig. 3), the associated thermal treatments (around 47% of the melting temperature for 6 h and 70% of the melting temperature for 1 h respectively) could act as an annealing step [40] of the PCL bundles, relieving the residual tensions and softening the material.

3.3.2 Environmental influence on the mechanical characteristics of the PNaSS grafted and non-grafted poly(ε-caprolactone) bundles

Considering that the knee joint reaches temperatures between 33˚C and 36.7˚C after 1h walking [41] the samples were immersed in water at 4 different temperature conditions: room temperature (25°C), 33, 37 and 40 °C (as severe inflammation situation). The results were compared to assays performed in air at room temperature (Table 2).

Table 2. Mechanical data obtained from traction experiments in aqueous media (n=5).

	Temperature	Young's M (MPa)	Elastic strain (%)	UTS (MPa)
Crudes bundles	Air (room temp)	961 ± 49	21 ± 2	353 ± 29
	25	923 ± 32	25 ± 2	323 ± 29
	33	901 ± 41	27 ± 3	276 ± 12
	37	843 ± 29	26 ± 1	329 ± 37
	40	798 ± 67	27 ± 1	313 ± 22
Bundles after thermal grafting	Air (room temp)	717 ± 64	31± 1	280 ± 17
	25	878 ± 99	26 ± 4	301 ± 15
	33	933 ± 39	24 ± 2	351 ± 6
	37	887 ± 79	24 ± 2	318 ± 30
	40	618 ± 83	28 ± 1	279 ± 14

These results confirm the viscoelastic behavior of the polymer [42] since the increase of the assays temperature will induce a reduction of Young modulus. The rise of the temperature weak the secondary bonds between the molecules and, by consequence, decrease the stress required to deform the material. For crude material the values varies almost linearly from 961 ± 49 to 798 ± 67 MPa (18 % reduction) at the highest temperature (40 °C). For the elastic strain and UTS, the environment seems to have a stronger influence than the temperature itself. From the lowest temperature (25°C) the elastic deformation was slightly increased and UTS decreased. Both properties oscillate between this temperature and 40 °C, finishing respectively at 27 ± 1 % (26 % higher) and 313 ± 22 MPa (11% lower).

Oppositely, when introduced in aqueous environment, PNaSS grafted samples experienced an increase of the Young modulus and a reduction of the elastic strain. However, this behavior, along with the UTS improvement, is not proportional as the temperature increased. The tendency seems to change after 33 °C, finishing with Young modulus and UTS both lower than at 25 °C and elastic strain slightly increased.

In general, it can be noted that for all three parameters the aqueous environment mitigates the differences between crude and PNaSS grafted samples and, most important, even at the most extreme conditions the surface modification will not menace the mechanical performance. The reversible deformation required for ACL for prosthesis applications is between 10 and 13% (the average strain of the ACL during walking) [43] and the UTS 38 MPa [44]. Even in the worst-case scenario the modified samples can easily respond these requirements with twice the strain and UTS 8 times higher than the native ACL.

3.3.3 Fatigue experiments

The final stress was determined for crude poly(ε-caprolactone)bundles, bundles after spin finish removal and PNaSS grafting (Table 3 and Fig 6).

Table 3. Mechanical data obtained from fatigue experiments (n=5).

	Final stress (%)			
Deformation	**10%**		**15%**	
Frequency	**3 Hz**	**5 Hz**	**3 Hz**	**5 Hz**
Crude bundles	15 ± 4	18 ± 0	10 ± 1	13 ± 4
Bundles without spin finish	33 ± 10	36 ± 10	20 ± 6	35 ± 14
Bundles after thermal grafting	49 ± 12	47 ± 13	13 ± 4	26 ± 22

As exhibited at Fig 6, crude samples submitted to the same deformation present similar behavior along with the assay, suggesting that this parameter has a stronger influence in the resistance loss than the frequency of the movement, which is natural as the prosthesis, would be more damaged with a 120 ° bending motion than a 90 ° bending. At the same time, these samples had an important loss of resistance throughout the test, finishing at 10 to 18% of the initial value.

In the case of fibers without spin finish components, samples had a lower loss of resistance (conserving between 20 and 36% of the initial resistance) and thermal grafted bundles presented the higher remaining resistance of the study (between 13 and 49% of the initial value). Once again the deformation length showed a strong influence on the results, however, the difference was much more pronounced for PNaSS grafted samples than for crude bundles.

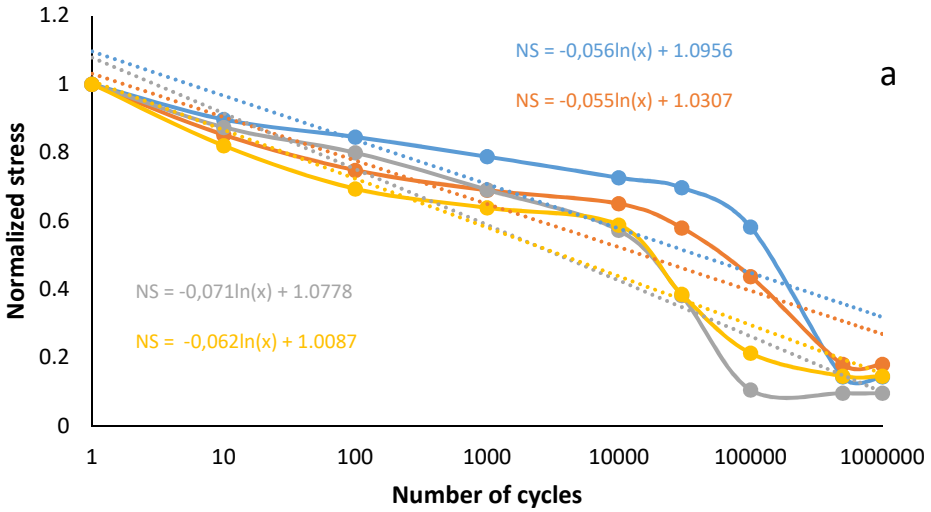
a
NS = -0,056ln(x) + 1.0956
NS = -0,055ln(x) + 1.0307
NS = -0,071ln(x) + 1.0778
NS = -0,062ln(x) + 1.0087
Normalized stress
Number of cycles
1.2
1
0.8
0.6
0.4
0.2
0
1
10
100
1000
10000
100000
1000000

355

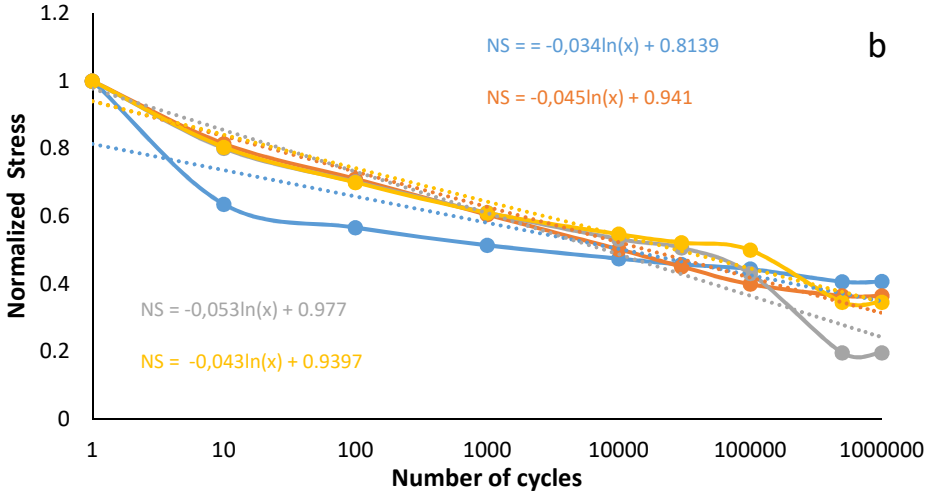
b
NS = = -0,034ln(x) + 0.8139
NS = -0,045ln(x) + 0.941
NS = -0,053ln(x) + 0.977
NS = -0,043ln(x) + 0.9397
Normalized Stress
Number of cycles
1.2
1
0.8
0.6
0.4
0.2
0
1
10
100
1000
10000
100000
1000000

356

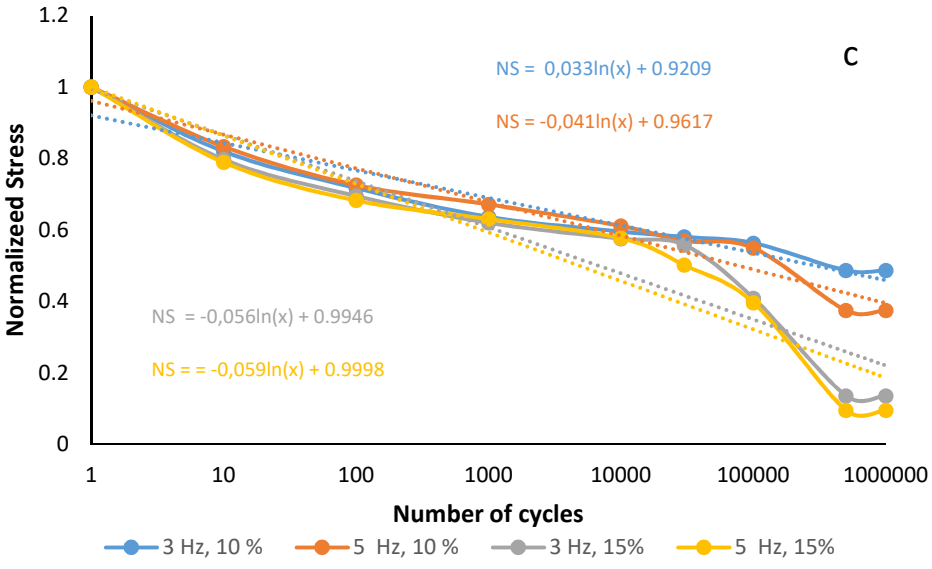
c
NS = 0,033ln(x) + 0.9209
NS = -0,041ln(x) + 0.9617
NS = -0,056ln(x) + 0.9946
NS = = -0,059ln(x) + 0.9998
Normalizeed Stress
Number of cycles
1.2
1
0.8
0.6
0.4
0.2
0
1
10
100
1000
10000
100000
1000000
3 Hz, 10 %
5 Hz, 10 %
3 Hz, 15%
5 Hz, 15%

357

Fig 6. Normalized S-N curves for fatigue experiments on a)crude poly(ε-caprolactone), b) poly(ε-caprolactone) after spin finish removal and c) grafted poly(ε-caprolactone) fibers (n=5).

Considering the results as a percentage, it's possible to convert these values on remaining stress for the samples after 1000, 100.000 and 1 million cycles. The values of stress (αf) for these three groups are exposed in the Table 4.

Table 4. Maximum and minimum values of the remaining stress for crude PCL samples, PCL after spin finish removal and thermal grafted PCL after 1000, 100.000 and 1 million cycles.

	Af (MPa)		
Number of cycles	**1000**	**100.000**	**1 million**
Crude bundles	276≤ αf ≤ 223	205≤ αf ≤ 39	60≤ αf ≤ 35
Bundles without spin finish	181≤ αf ≤ 151	149≤ αf ≤ 116	107≤ αf ≤ 56
Bundles after thermal grafting	187≤ αf ≤ 173	157≤ αf ≤ 112	134≤ αf ≤ 36

With the aforementioned UTS value of natural ligament in mind, all the studied conditions will present at least a resistance similar to the human ACL, even in the extreme case of 1million cycles. However, in a more practical scenario a valuable information can be drawn from the evolution of the fatigue behavior. Even though the crude samples presents higher stress values after the first 1000 cycles, they suffer the stronger reduction compared to the other groups, reaching very low stress levels already after 100.000 cycles. Once again, this different behavior between crude samples and after "thermal treatments" can be linked to reduction of the residual stress, which was reported to accelerate fatigue damage [45].

3.3.4 Walk Cycle experiments

After a 30 minutes cycle of walk the PCL samples were subject to tensile tests, the main mechanical properties were determined and compared to results obtained without walking simulation. The figure 7 shows the typical aspect of the curves and the results are detailed in table 5.

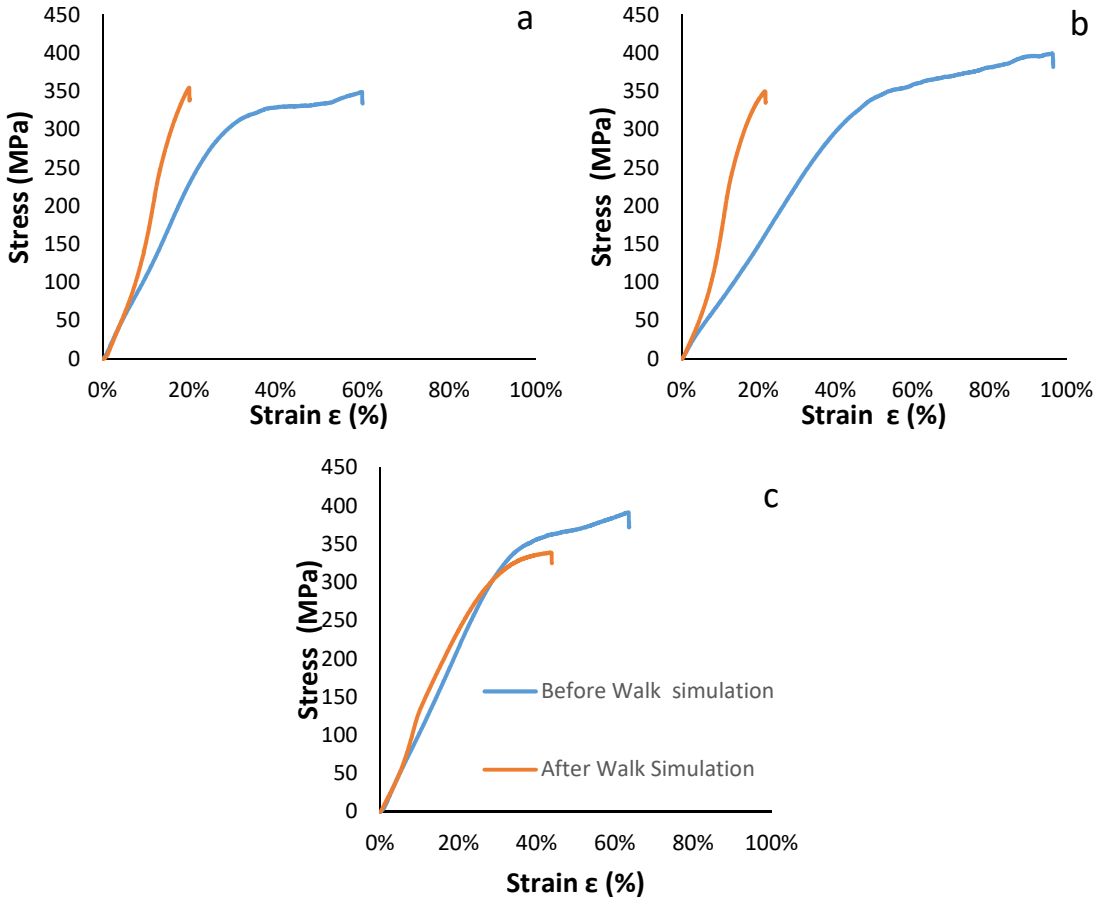

Fig 7. Stress-strain curves for tensile experiments before and after simulated walk for a) crude, b) after spin finish removal and c) grafted poly(ε-caprolactone) fibers .

The general behavior of the samples was typical of semi-crystalline polyester with both linear and non-linear elastic region [29] suffering strain-hardening in all three conditions. This phenomenon takes place during the walking simulation test. In order to keep the pace of the walking, during the simulation the samples were stretched with a much higher strain rate than used during the tensile tests inducing an increase of the Young modulus of the samples [46].

Table 5. Mechanical data obtained from walk cycle experiments (n=5).

		Young modulus (MPa)	Elastic strain (%)	Ultimate tensile strain (MPa)
Crude bundles	Before walk	961 ± 49	21 ± 2	353 ± 29
	After walk	1361 ± 56	12 ± 1	340 ± 29
Bundles without spin finish	Before walk	789 ± 60	28 ± 1	297 ± 32
	After walk	1220 ± 136	12 ± 0	360 ± 17

Bundles after thermal grafting	Before walk	717 ± 64	31 ± 1	280 ± 17
	After walk	1147 ± 56	12 ± 1	333 ± 8

391

392 Crude bundle's Young modulus varies from 961 to 1361 MPa (41% increase)
393 and the elastic strain from 21 to 12 (43% reduction). It's important to notice that in the
394 curve after walk (Fig 7a) the UTS value was not significantly changed, however the
395 rupture occurs just after the elastic zone, showing almost no plastic deformation.

396 For bundles without spin finish, the Young modulus has an increase from 789 to
397 1220 (54% increase) and the elastic strain decreased from 28 to 12 (55% decrease).
398 Once again almost no plastic zone was verified (Fig 7b).

399 Bundles after thermal grafting showed similar behavior, with Young modulus
400 increasing 59% and elastic strain decreasing 61%. Yet, contrarily to the two previous
401 conditions, a small plastic zone can be noticed before the rupture (Fig 7c) and at 300
402 MPa the sample showed almost 40% deformation without rupture. Naturally, the
403 material should operate in the elastic zone, however, since the elastic strain of all
404 conditions are close to the minimum required such toughness improvement could be an
405 interesting edge against prosthesis failure.

406 ## 4. Conclusion

407 The study aimed to demonstrate that poly(caprolactone) fibers can present
408 suitable mechanical properties to native ACL replacement after surface
409 functionalization. This goal was achieved by different mechanical assays, trying to
410 approach the conditions of the natural ligament daily efforts. The results indicate that, in
411 addition to the already recognized biological response enhancement brought by this
412 procedure, the "thermal treatment" inherent to this functionalization technique create a
413 desirable side effect that can improve the ability of the PCL fibers to adapt to different

environments and mechanical demands. Therefore, the combination of the results justifies the interest of the choice of poly(ε-caprolactone) for the elaboration of ligament prosthesis with appropriate mechanical behavior

Conflict of interest

The authors declare that they have no known competing financial interests or personal relationships that could have appeared to influence the work reported in this paper.

Credit authorship contribution statement

Andre Rangel: Investigation, Formal analysis, Methodology, Writing - original draft. Laila Colaço: Investigation, Writing - original draft. Ngoc Tuan Nguyen: Investigation, Formal analysis. Jean-François Grosset: Conceptualization, Formal analysis, Methodology. Christophe Egles: Conceptualization, Formal analysis, Resources, Supervision, Writing - review & editing. Veronique Migonney: Conceptualization, Formal analysis, Funding acquisition, Methodology, Project administration, Supervision, Validation, Writing - review & editing.

Acknowledgments

The authors would like to thanks Marine Ferreira, MDB Texinov and LARS SA for the technical support and the French Public Investment Bank and the French state – PSPC application – for the financial support of Liga2bio project.

References

[1] Walters M A, Chambers M C, Karki R, Knox E, Levengood G, El-Amin S. Anterior Cruciate Ligament Tissue Engineering: A Review of Current Investigations. Journal of Nanotechnology and Material Science. 2016

[2] Marieswaran M, Jain I, Garg B, Sharma V, Kalyanasundaram D, “A Review on Biomechanics of Anterior Cruciate Ligament and Materials for Reconstruction,” Applied Bionics and Biomechanics, vol. 2018, pp. 1–14, 2018.

[3] Jamil T, Ansari U, Najabat Ali M, Mir M, “A Review on Biomechanical and Treatment Aspects Associated with Anterior Cruciate Ligament,” IRBM, vol. 38, no. 1, pp. 13–25, 2017.

[4] Legnani C, Ventura A, Terzaghi C, Borgo E, Albisetti W. Anterior cruciate ligament reconstruction with synthetic grafts. A review of literature. International Orthopaedics (SICOT) 34, 465–471, 2010.

[5] Vieira A C, Guedes R M, Marques A T, “Development of ligament tissue biodegradable devices: A review,” Journal of Biomechanics, vol. 42, no. 15, pp. 2421–2430, 2009.

[6] Parchi P D, Gianluca C, Dolfi L, Baluganti A, Nicola P, Chiellini F, Lisanti M. Anterior cruciate ligament reconstruction with LARS™ artificial ligament results at a mean follow-up of eight years. Int Orthop. 37(8):1567-1574, 2013.

[7] Iliadis D P, Bourlos D N, Mastrokalos D S, Chronopoulos E, Babis G C. LARS Artificial Ligament Versus ABC Purely Polyester Ligament for Anterior Cruciate Ligament Reconstruction. Orthop J Sports Med. 4(6):2325967116653359, 2016.

[8]Smedt M D. Les prothèses du ligament croisé antérieur : analyse d’un échec. Acta Orthopaedica Belgica, Vol. 64, 1998.

[9] Viateau V, Manassero M, Anagnostou F, Guérard S, Mitton D, Migonney V. Biological and Biomechanical Evaluation of the Ligament Advanced Reinforcement System (LARS AC) in a Sheep Model of Anterior Cruciate Ligament Replacement: A 3-Month and 12-Month Study. Arthroscopy: The Journal of Arthroscopic & Related Surgery, 29: 1079-1088, 2013.

[10] Teuschl A, Heimel P, Nürnberger S, van Griensven M, Redl H, Nau T. A Novel Silk Fiber-Based Scaffold for Regeneration of the Anterior Cruciate Ligament: Histological Results From a Study in Sheep. Am J Sports Med. 44(6):1547-1557, 2016.

[11] Altman G H, Horan R L, Lu H, Moreau J, Martin I, Richmond J C, Kaplan D L. Silk matrix for tissue engineered anterior cruciate ligaments, Biomaterials, 4131-4141, Volume 23, Issue 20, 2002.

[12] Cooper J A Jr, Sahota J S, Gorum W J 2nd, Carter J, Doty S B, Laurencin C T. Biomimetic tissue-engineered anterior cruciate ligament replacement. Proc Natl Acad Sci U S A. 104(9):3049-3054, 2007.

[13] Lu H, Cooper J A, Manuel S, Freeman J W, Attawia M A, Ko F K, Laurencin C T. Anterior cruciate ligament regeneration using braided biodegradable scaffolds: in vitro optimization studies, Biomaterials, Volume 26, Issue 23, Pages 4805-4816, 2005

[14] Ferreira F N, Alves N M, Paiva M C, Silva M. Biodegradable polymer nanocomposites for ligament/tendon tissue engineering. Journal Of Nanobiotechnology, 18, 23, 2020

[15] Yahia L, Hagemeister N, Drouin G, Rivard C H, Rhalmi S, Newman N Evaluation of Cruciate Ligament Prostheses — Critique of Current Concepts and Procedures. In: Yahia L. (eds) Ligaments and Ligamentoplasties. Springer, Berlin, Heidelberg, 1997.

[16] Leong N L, Petrigliano F A, McAllister D R. Current tissue engineering strategies in anterior cruciate ligament reconstruction. J Biomed Mater Res A. 102(5):1614-1624, 2014.

[17] Leroux A, Maurice E, Viateau V, Migonney V. Feasibility Study of the Elaboration of a Biodegradable and Bioactive Ligament Made of Poly(ε-caprolactone)-pNaSS Grafted Fibers for the Reconstruction of Anterior Cruciate Ligament: In Vivo Experiment, IRBM, 38-44, Volume 40, Issue 1, 2019.

[18] Pitt C, Chasalow F, Hibionada Y, Kilmas D, Schindler A. Aliphatic polyesters. I. The degradation of poly(E-caprolactone) in vivo. Journal of Applied Polymer Science, 26: 3779-3787, 1981.

[19] Sun H, Mei L, Song C, Cui X, Wang P. The in vivo degradation, absorption and excretion of PCL-based implant. Biomaterials, 27: 1735-1740, 2006.

[20] Höglund A, Hakkarainen M, Albertsson A. Degradation profile of poly(E-caprolactone) - the influence of macroscopic and macromolecular biomaterial Design. Journal of Macromolecular Science, Part A, 44: 1041-1046, 2007.

[21] Azimi B, Nourpanah P, Rabiee M, Arbab S. Poly(E-caprolactone) Fiber: An Overview. Journal of Engineered Fiber and Fabrics, 2014.

[22] Ratner B D, Hoffman A S, Schoen F J, Lemons J E. "Introduction - Biomaterials Science: An Evolving, Multidisciplinary Endeavor." In :Biomaterials Science: An Introduction to Materials: Third Edition, 2013.

[23] Belleney J, Helary G, Migonney V. Terpolymerization of methyl methacrylate, poly(ethylene glycol) methyl ether methacrylate or poly(ethylene glycol) ethyl ether methacrylate with methacrylic acid and sodium styrene sulfonate: determination of the reactivity ratios. European Polymer Journal, 38: 439-444, 2002.

[24] Felgueiras H, Migonney V. Sulfonate groups grafted on Ti6Al4V favor MC3T3-E1 cell performance in serum free medium conditions. Materials Science and Engineering C, 39: 196-202. doi:PMID: 17929865, 2014.

[25] Amokrane G, Humblot V, Jubeli E, Yagoubi N, Ramtani S, Migonney V, Falentin-Daudré C. Electrospun Poly(ε-caprolactone) Fiber Scaffolds Functionalized by the Covalent Grafting of a Bioactive Polymer: Surface Characterization and Influence on in Vitro Biological Response. ACS Omega 4 (17), 17194-17208, 2019

[26] Rohman G, Huot S, Vilas-Boas M, Radu-Bostan G, Castner D G, Migonney V. The grafting of a thin layer of poly(sodium styrene sulfonate) onto poly(ε-caprolactone) surface can enhance fibroblast behavior. J Mater Sci: Mater Med 26, 206, 2015.

[27] Pavon-Djavid G, Gamble L, Ciobanu M, Gueguen V, Castner D, Migonney V. Bioactive Poly(ethylene terephtalate) Fibers and Fabrics: Grafting, Chemical Characterization and Biological Assessment . Biomacromolecules, 8: 3317-3325. 2007.

[28] Brulez B, Laboureau J P, Migonney V, Ciobanu M, Pavon-Djavid G, Siove A. Biomimetic Prosthetic Ligament and Production Method Thereof. United States Patent No.: US 7,700,147 B2, 2004.

[29] Leroux A, Egles C, Migonney V. Impact of chemical and physical treatments on the mechanical properties of poly(ε-caprolactone) fibers bundles for the anterior cruciate ligament reconstruction. PLoS ONE 13(10): e0205722, 2018.

[30] Helary G, Noirclere F, Mayingi J, Migonney V. A new approach to graft bioactive polymer on titanium implants: Improvement of MG 63 cell differentiation onto this coating. Acta Biomaterialia 5, p. 124–133, 2009.

[31] Kweon H Y, Yoo M K, Park I K, Kim T H, Lee H C, Lee H, Oh J, Akaike T, Cho C. A novel degradable polycaprolactone networks for tissue engineering, Biomaterials, vol. 24, no. 5, pp. 801–808, 2003.

[32] Woodruff, M. A. Hutmacher D. M. The return of a forgotten polymer—Polycaprolactone in the 21st century, Progress in Polymer Science, Volume 35, Issue 10, Pages 1217-1256, 2010.

[33] Hollis J M, Takai S, Adams D J, Horibe S, Woo S L-Y. The effects of knee motion and external loading on the length of the anterior cruciate ligament (ACL): A kinematic study. Journal of Biomechanical Engineering, vol 113, 208 – 214, 1991.

[34] Gasq D, Moliner F, Lafosse J-M. Physiologie, méthodes d'explorations et troubles de la marche. Facultés de Médecine de Toulouse, 2013.

[35]Dutton M. Dutton's orthopaedic examination evaluation and intervention. McGraw-Hill Medical, 2012.

[36] Gao X, Hao F, Huang Z, Fang D. Mechanics of adhesive contact at the nanoscale: The effect of surface stress. International Journal of Solids and Structures, v51, I3-4, 566-574, 2014.

[37] Dekkar D, Bénédic F, Falentin-Daudré C, Rangel A, Issaoui R, Migonney V, Achard J; Microstructure and biological evaluation of nanocrystalline diamond films deposited on titanium substrates using distributed antenna array microwave system., Diamond and Related Materials, Volume 103, 2020.

[38] Hornberger L E, Devries K L. The effects of residual stress on the mechanical properties of glassy polymers. Polym Eng Sci, 27: 1473-1478, 1987.

[39] So P, Broutman L J. Residual stresses in polymers and their effect on mechanical behavior. Polym Eng Sci, 16: 785-791, 1976.

[40] Farah S, Anderson D, Langer R. Physical and mechanical properties of PLA, and their functions in widespread applications - A comprehensive review. Advanced Drug Delivery Reviews, 107: 376-392, 2016.

[41] Abdel-Sayed P, Darwiche S, Kettengerger U, Pioletti D. The role of energy dissipation of polymeric scaffolds in the mechanobiological modulation of chondrogenic expression. Biomaterials, 35: 1890-1897, 2014.

[42] Noroozi N, Thomson J, Schafer L, Hatzikiriakos S. Viscoelastic behavior and flow instabilitites of biodegradable poly(ε-caprolactone) polyesters. Rheologica Acta, 51: 179-192, 2012.

[43] Taylor K, Cutcliffe H, Queen R, Uttukar G, Spritzer C, Garret W. In vivo measurement of ACL length and relative strain during walking. Journal of Biomechanics, 46: 478-483, 2013.

[44] Pauly H M, Kelly D J, Popat K C, Trujillo N A, Dunne N J, McCarthy H O, Donahue T L H. Mechanical properties and cellular response of novel electrospun nanofibers for ligament tissue engineering: Effects of orientation and geometry. Journal of the Mechanical Behavior of Biomedical Materials,Volume 61, 258-270, 2016.

[45] Koch I, Just G, Brod M, Chen J, Doblies A, Dean A, Gude M, Rolfes R, Hopmann C, Fiedler B. Evaluation and Modeling of the Fatigue Damage Behavior of Polymer Composites at Reversed Cyclic Loading. Materials (Basel). 12(11):1727, 2019.

[46] Siviour C R, Jordan JL. High Strain Rate Mechanics of Polymers: A Review. J. dynamic behavior mater. 2, 15–32, 2016.

Biodegradable synthetic ligament

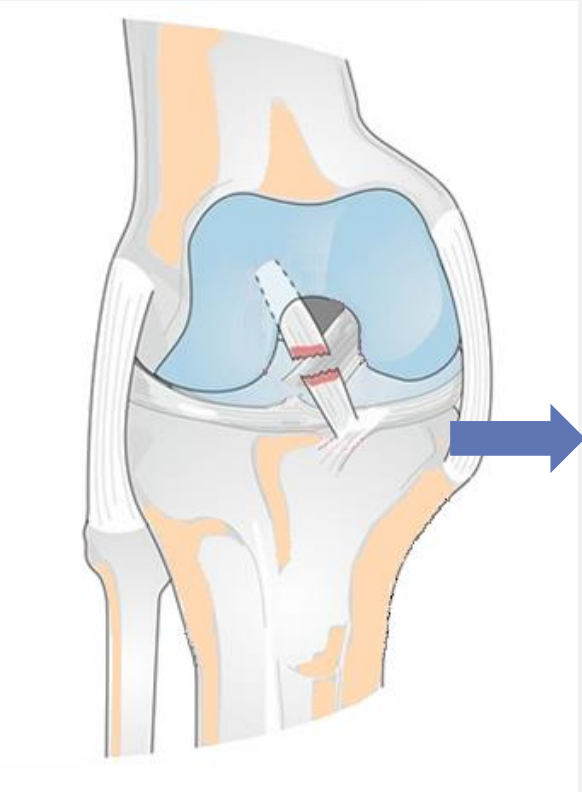

ACL rupture

bioactive polymer grafting

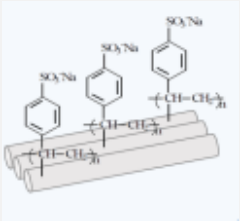

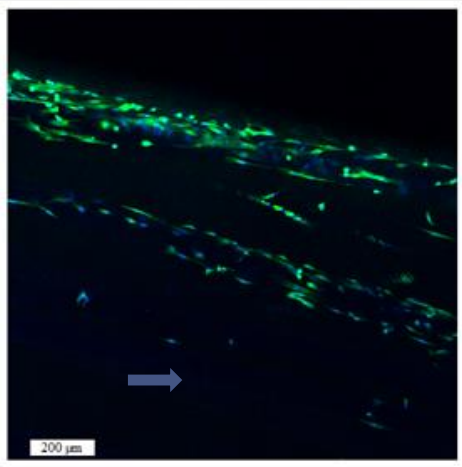

cell colonization

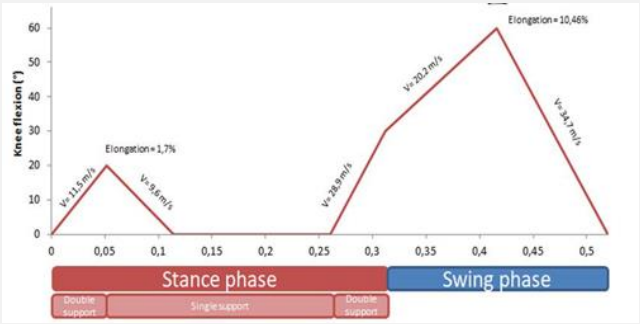

mechanical properties/daily activities